Int J Physiol Pathophysiol Pharmacol 2018;10(2):105-114
www.ijppp.org /ISSN:1944-8171/IJPPP0076397

Original Article

Tumor associated macrophages deliver iron to tumor cells via Lcn2

Xiaoyue Duan, Kun He, Jing Li, Man Cheng, Hongjiao Song, Jinqiu Liu, Ping Liu

School of Biomedical Engineering and Med-X Research Institute, Shanghai Jiao Tong University, Shanghai, People's Republic of China

Received March 20, 2018; Accepted April 2, 2018; Epub April 20, 2018; Published April 30, 2018

Abstract: Cancer cells exhibit an increasing iron demand associated with the tumor progression. But the mechanism of iron accumulation in the tumor microenvironment is still unclear. Tumor associated macrophages (TAMs) in the tumor microenvironment may act as extra iron source. However, evidence is still lacking in TAMs as iron donors. In the present study, we found that iron concentration was significantly increased at tumor metastatic stage, which could be attributed to up-regulated expression of lipocalin2 (Lcn2). TAMs in the microenvironment secreted Lcn2. Moreover, TAMs increased intracellular iron concentration in tumor cells via Lcn2 as transporter, which could be restored by Lcn2 antibody neutralization. In conclusion, TAMs increased intracellular iron concentration of the tumor cells via Lcn2 which acted as an iron transporter. Targeting Lcn2 secretion in TAMs to "starve cancer cells" could act as alternative option for tumor therapy.

Keywords: Iron, tumor associated macrophages, Lcn2, breast cancer

Introduction

More recently, it has been suggested that a wide spectrum of human cancers can be viewed as iron-overload diseases [1]. For instance, large sample studies have demonstrated that in sera of breast cancer patients, ferritin and transferrin expression are higher than that in healthy people [2]. And some studies have shown that breast cancer cells display enhanced iron sequestration capacity compared with that in non-neoplastic cells, which is associated with aggressive tumor growth in mice and is correlated with poor outcomes in humans [3]. In addition, it has been directly revealed by synchrotron radiation X-ray fluorescence (SXRF) imaging that iron concentration in malignant tissues is higher than that in benign lesions and normal tissues [4]. In addition, recent researches have shown that iron in the tumor microenvironment is correlated with tumor metastasis [3, 5]. Moreover, it has been pointed out that iron may play a more prominent role in tumor metastasis [6]. However, the source of extra iron in tumor cells is still unrevealed.

Tumor-associated macrophages (TAMs) that closely resemble alternatively (M2)-polarized macrophages are major players in the tumor microenvironment [7]. Furthermore, an increasing body of evidence has indicated that patients with higher TAMs density have significantly worse clinical outcomes [8]. The gene expression profile of iron metabolism is strikingly different in classically (M1) and alternatively (M2) polarized macrophages--two extremes of the polarization spectrum [9]. M1 macrophages are characterized by ferritin^{high}/ferroportin (Fpn)^{low} phenotype, which tend to store iron. M2 macrophages are characterized by elevated heme uptake and degradation, as well as ferritin^{low}/Fpn^{high} phenotype, which are believed to recirculate iron to the microenvironment [10]. Recent studies have suggested that Lipocalin2 (Lcn2), an alternative iron transporter, mediates a new iron-delivery pathway [6, 11, 12]. Jung et al. have reported an increased expression of Lcn2 in TAMs [13]. Whether TAMs act as a source to provide tumor cells with extra iron through Lcn2 is of interest.

In this study, we used the 4T1 murine breast cancer model to mimic late stage breast cancer

[14, 15], and studied the interrelations of iron concentration, TAMs and Lcn2 in the tumor metastasis. Our results demonstrated that TAMs in the tumor microenvironment secreted Lcn2. Furthermore, TAMs could traffic iron via Lcn2 to tumor cells and increase cellular iron concentration.

Material and methods

Ethics statement

All animal experiments were approved by the Animal Welfare Committee of Shanghai Jiao Tong University.

Cell culture

The 4T1 and 67NR murine breast carcinoma cell lines were a gift from Prof. Qian Huang, Shanghai First People's Hospital, affiliated to Shanghai Jiao Tong University [16]. Cells were maintained with DMEM (Hyclone, USA) supplemented with 10% fetal bovine serum and 100 mg/L penicillin/streptomycin. Cells were maintained in a 37°C incubator with humidified 5% CO_2.

Breast cancer animal model

6-8 weeks old, female BALB/c mice were purchased from the Slac Laboratory Animal. Iron-overloaded mice were achieved by intraperitoneal injection of 100 μg iron dextran (Sigma Aldrich) every third day for 4 weeks. For the subcutaneous breast cancer model, 4T1 breast cancer cells (1×10^6) were injected subcutaneously into the dorsal part of the right thigh. Mice were sacrificed by cervical vertebra luxation 14 days post injection. Tumor tissues were harvested and frozen until use. For the in situ breast cancer model, 5×10^5 4T1 cells were injected into the fourth fat pad. For experimental metastasis, mice were anesthetized and 1×10^5 4T1 cells were injected intravenously. Mice were sacrificed, and lungs were harvested and fixed with Bowie's solution. Deferoxamine (DFO) was administrated by regional subcutaneous injection with 10 mg DFO per mouse per day after tumor inoculation. Mice were sacrificed 14 days after tumor inoculation. Tumor tissues were collected, weighed, and frozen stored at -80°C.

Tumor metastasis observed using Micro PET/CT

Micro PET/CT scanning was performed using an Inveon system (Siemens Preclinical Solutions). On day 10, 14 and 21 after tumor inoculation, tumor-bearing mice were anesthetized by intraperitoneal injection of pentobarbital sodium, followed by intravenous injection of 18F-FDG, and were then scanned to verify the tumor metastasis in vivo.

Preparation of cryosections

The frozen tumor tissues were sliced into 20 μm in thickness at -20°C (LEICA CM1900, Germany), and mounted on the 3525 Ultralene XRF film (SPEX CertiPrep, Metuchen, NJ), air-dried. In addition, several adjacent sections of the same thickness were placed on microscopic slides and used for immunohistochemical analysis and immunofluorescent staining. Tissue sections were stored frozen until use.

Synchrotron radiation X-ray fluorescence elemental mapping

Synchrotron radiation X-ray fluorescence imaging was performed at the BL15U beamline of Shanghai Synchrotron Radiation Facilities (SSRF), China. The X-ray energy used for elements mapping was 12 keV and the spot size was 100 μm. X-ray fluorescence emission was collected by an energy-dispersive Li-ion drifted detector [seven-element Si (Li) detector, E2V].

Preparation of tissue lysates, secretory protein and western blot assay

Tissues stored at -80°C were lysed in RIPA lysis buffer (with cocktail proteinase inhibitor, 0.1% SDS and added phenylmethylsulfonyl fluoride (PMSF) to 1 mM), and incubated on ice for 4 hours. Western blot analysis was performed using primary antibodies for TfR (Abcam, 1:1000), Lcn2 (Millipore, 1:200) and actin (Beyotime, 1:1000), and detected using the appropriate HRP-labelled secondary antibody (KPL, 1:2000) and enhanced chemiluminescence (Pierce). In addition, the culture medium was collected and used to determine Lcn2 secretion by western blot analysis. Western blot shown was representative of three separate experiments.

Immunohistochemical and immunofluorescent analysis

For immunohistochemical staining, frozen tumor sections were fixed for 10 minutes in cold acetone, then peroxidase quenched with 0.3% H_2O_2 in 99.7% methanol, washed in PBS and blocked for 30 minutes with 5% Bovine Serum Albumin (BSA). Lcn2 Primary antibody (rabbit anti mouse Lcn2 antibody, Sino biological Inc.) or isotype rabbit IgG (Sino biological Inc.) was applied overnight at 4°C in PBS, followed by three washes in PBS, and then biotinylated secondary antibody, streptavidin-HRP and diaminobenzidine (DAB) peroxidase substrate were added. Nuclei were counterstained with hematoxylin.

For immunofluorescent staining, frozen tumor sections were fixed in cold acetone for 10 minutes, and air dried for 15 minutes, washed three times in cold PBS and then blocked for 30 minutes in PBS with 5% BSA. To identify TAMs, primary antibody FITC labeled-CD68 (Biolegend, 1:200) was applied overnight at 4°C, followed by washes three times in PBS. To detect the expression of Lcn2, primary anti-Lcn2 antibody (Millipore, 1:200) was applied overnight at 4°C, followed by washes three times in PBS. Then, the samples were incubated with NL557 conjugated anti-rabbit secondary antibody (R&D systems, 1:200) for 1 hour at room temperature, followed by washes three times in PBS. Nuclei were counterstained with DAPI in mounting medium (VECTASHELD®, Vector). The slices were viewed using confocal microscopy (Leica TCS SP5).

Flow cytometry analysis of CD68 positive TAMs and TAMs separation

Fresh tumor tissue was sectioned and chopped into small pieces and single cell suspensions were obtained using GentleMACS Dissociator (Miltenyl Biotec). For flow cytometry analysis of CD68 positive cells, anti-mouse CD68-PE antibody was used to label TAMs. For TAMs separation, single cell suspension was separated using Stemcell® PE-separation kit and anti-mouse CD68-PE antibody. The sorted TAMs were maintained in DMEM supplemented with 10% FBS. For conditioned medium collection, TAMs were cultured in 10 cm petri dish with DMEM supplemented with 10% FBS for 24 hours. Culture medium was replaced with serum-free medium and conditioned medium was collected after 24 hours.

ICP/MS detection of iron concentration

0.4 μm pore size transwell chambers (Costar Corporation) were used to avoid direct contact between 4T1 cells and TAMs. TAMs sorted from subcutaneous 4T1 breast cancer tissues were seeded in the lower chamber. 5×10^4 4T1 cells or 67NR cells were added in the upper chamber and incubated with TAMs for 24 h, respectively. Iron concentration in TAMs, 4T1, and 67NR cells was detected using ICP/MS (Element R., Thermo Fisher Scientific, Germany).

To detect whether some molecules secreted into medium could alter cellular iron concentration of 4T1 cells in the upper chambers, in the control group, only DMEM was added into lower chambers. 25% and 50% conditioned medium from TAMs mixed with DMEM was loaded into lower chamber separately. In the TAMs group, sorted TAMs were seeded into lower chamber. To verify the secreted Lcn2, Lcn2 primary antibody or isotype rabbit IgG was added to lower chambers. After 24 hours of incubation, 4T1 cells were collected and lysed by 1% high-quality nitric acid which was diluted with deionized distilled water. For quantification of iron concentration in tumor tissues, tumor tissues were chopped into small pieces and stable solution was obtained by nitrolysis with high-quality nitric acid. Iron concentration was detected using ICP/MS.

Lcn2 treatment

Recombinant mouse Lcn2 protein (Sino biological Inc.) was diluted in distilled water (Watsons, containing no iron) at final concentration of 5 uM and 10 uM. For holo-Lcn2, 1 ul $FeCl_3$ (40 mM) was added into 50 ul 5 uM and 10 uM Lcn2 solution respectively. The mixtures were kept for 10 min at room temperature. Ultracentrifugation was performed to eliminate unbounded iron. Lcn2 solution without $FeCl_3$ treatment was referred as apo-Lcn2. Iron content in apo-Lcn2 and holo-Lcn2 was detected by ICP/MS. 50 ul of apo-Lcn2 and holo-Lcn2 was added into culture media of 4T1 cells. 1×10^5 4T1 cells were collected and intracellular iron concentration was detected by ICP/MS.

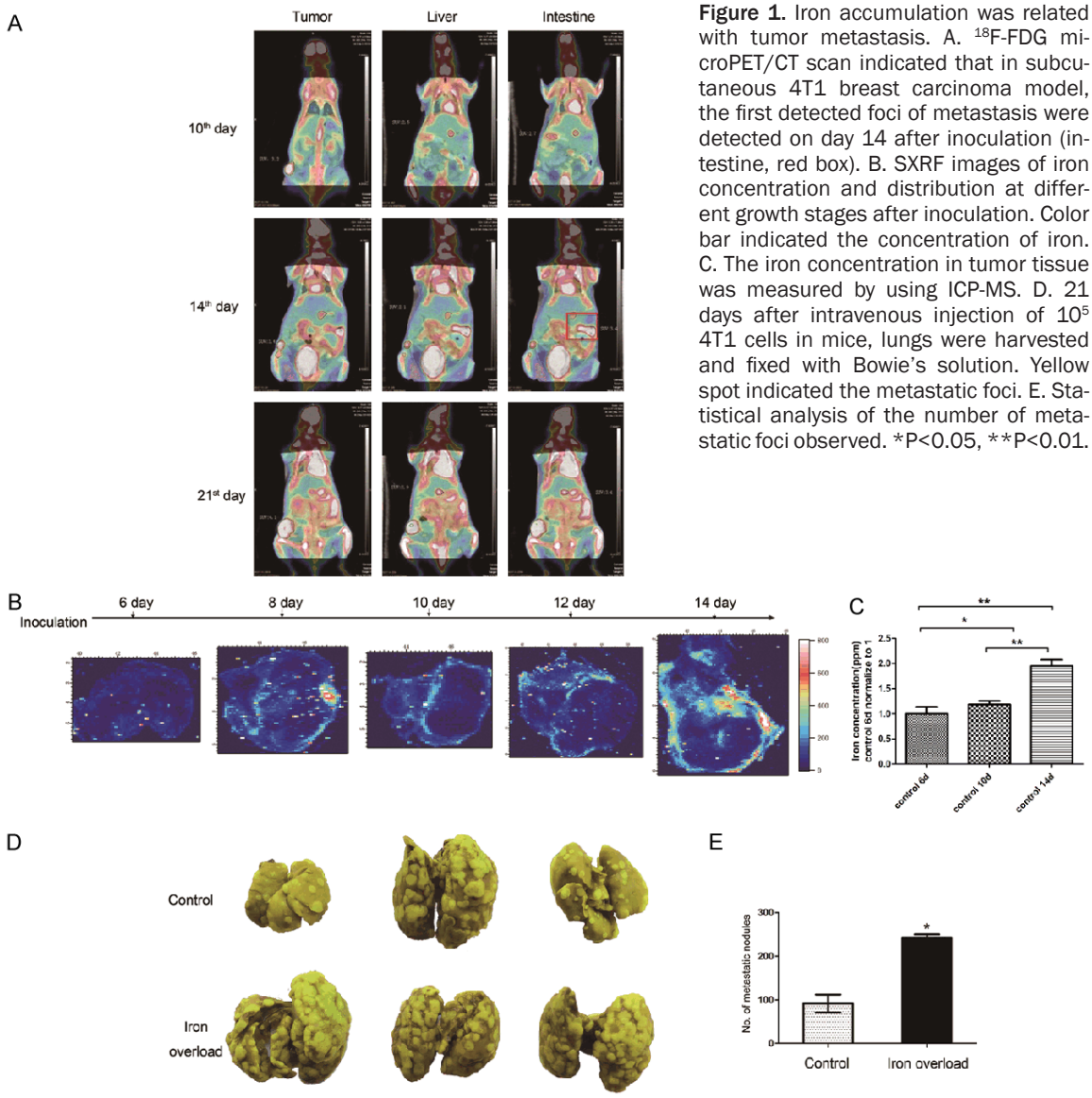

Figure 1. Iron accumulation was related with tumor metastasis. A. ^{18}F-FDG microPET/CT scan indicated that in subcutaneous 4T1 breast carcinoma model, the first detected foci of metastasis were detected on day 14 after inoculation (intestine, red box). B. SXRF images of iron concentration and distribution at different growth stages after inoculation. Color bar indicated the concentration of iron. C. The iron concentration in tumor tissue was measured by using ICP-MS. D. 21 days after intravenous injection of 10^5 4T1 cells in mice, lungs were harvested and fixed with Bowie's solution. Yellow spot indicated the metastatic foci. E. Statistical analysis of the number of metastatic foci observed. *P<0.05, **P<0.01.

Statistical analysis

The data were expressed as mean ± SD and were analyzed using student t test with P<0.05 as statistical significant. The statistical analysis was performed using Graphpad prism 5 software.

Results

Iron accumulation was correlated with tumor metastasis

In previous study, we demonstrated that among three kinds of trace elements studied, iron concentration was changed significantly at different tumor growth stages [17]. To evaluate iron concentration in tumor tissues at the time point of metastasis, tumor metastatic pattern of subcutaneous 4T1 murine breast cancer model was examined by Micro PET/CT. Tumor-bearing mice were separately scanned on day 10, 14 and 21 after tumor inoculation, respectively. As shown in **Figure 1A**, no metastasis foci were observed on day 10. Along with primary tumor growth, metastasis foci were detected in intestine on day 14 (**Figure 1A**, red box). On day 21, several metastasis foci were found in liver and intestine. Collectively, metastasis in 4T1 murine breast cancer model occurred 14 days after tumor inoculation. In the following study, iron concentration in tumor tissues at different time points was analyzed.

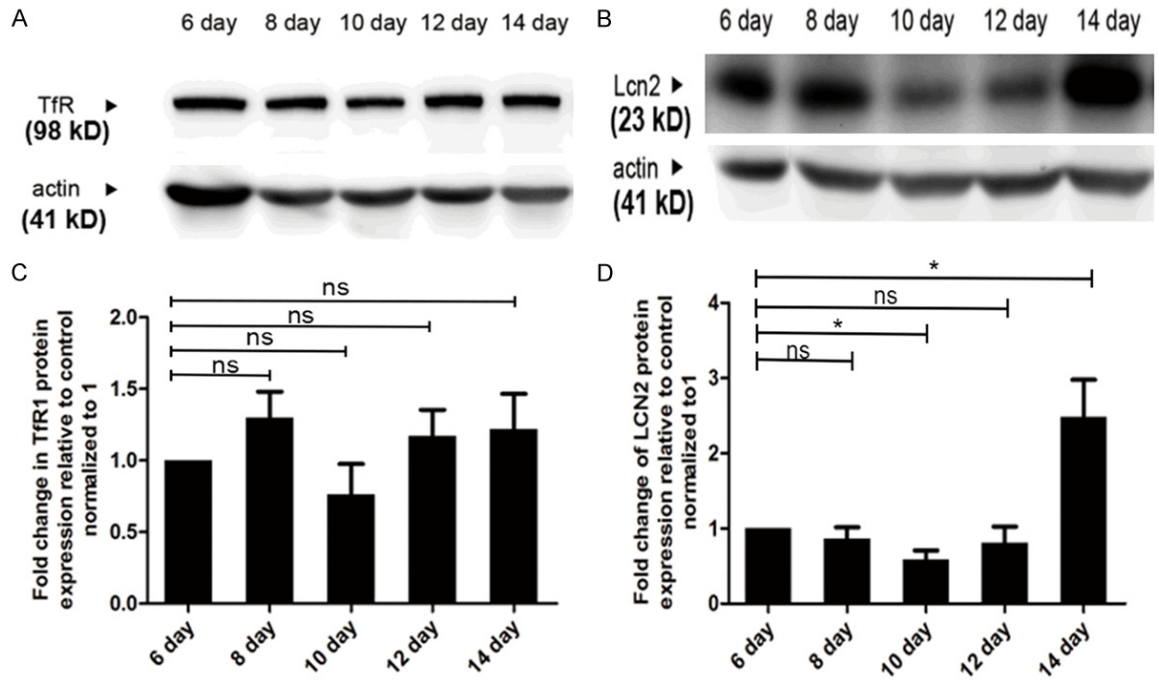

Figure 2. Lcn2 could potentially mediate iron accumulation at tumor metastasis stage. A-D. Western blot analysis of TfR and Lcn2 from tumor tissues, and their statistic. *P<0.05 by two way ANOVA.

SXRF mapping was utilized to study iron concentration and distribution in tumor tissues (**Figure 1B**). It was shown that iron concentration in tumor tissues on day 6 was basically the same level as background, which was indicated as base level. Then it was markedly increased on day 8. From day 8 to day 12, iron concentration was fluctuated in a narrow range. When metastatic foci were detected on day 14 after tumor inoculation, iron concentration in tumor tissues was drastically increased as compared to the base level. Furthermore, iron was generally localized in the peripheral region of tumor tissues in line with tumor invasive edge. The iron concentration in tumor tissues, measured by using ICP/MS, was increased gradually with tumor growth, as supported by the finding that iron concentration in tumor tissues on day 14 after tumor inoculation was markedly higher than that on day 6, 10 after tumor inoculation (**Figure 1C**). To further study the correlation of iron and tumor metastasis, we established the systemic iron-overloaded mice model by intraperitoneal injection of iron dextran every third day for 4 weeks before tumor inoculation. The markedly increased metastatic foci were observed in the lungs of iron-overloaded mice compared with that of the control group (**Figure 1D**, **1E**). Taken together, the above results indicated that iron plays a pivotal role in tumor metastasis.

Lcn2 could potentially mediate iron accumulation at tumor metastatic stage

Since transferrin receptor (TfR) has been commonly considered as the main mediator of iron internalization, the expression of TfR was studied at tumor metastatic stage. Western blot analysis showed that the expression of TfR in tumor tissues was only slightly changed at different time points (**Figure 2A**, **2B**). Even when tumor was about to metastasize, TfR expression in tumor tissues was stable from day 12 to day 14, which indicated that TfR was not the main contributor of iron accumulation in this event.

Iron delivering via Lcn2, which is considered to be related to tumor metastasis and serves as the shuttle transporter for numerous substances including iron, is normally in response to inflammatory cytokines and ER stress [18]. In this study, the expression of Lcn2 in tumor tissues was detected by western blot analysis. As shown in **Figure 2C**, **2D**, on day 14 after tumor inoculation, the expression of Lcn2 was greatly

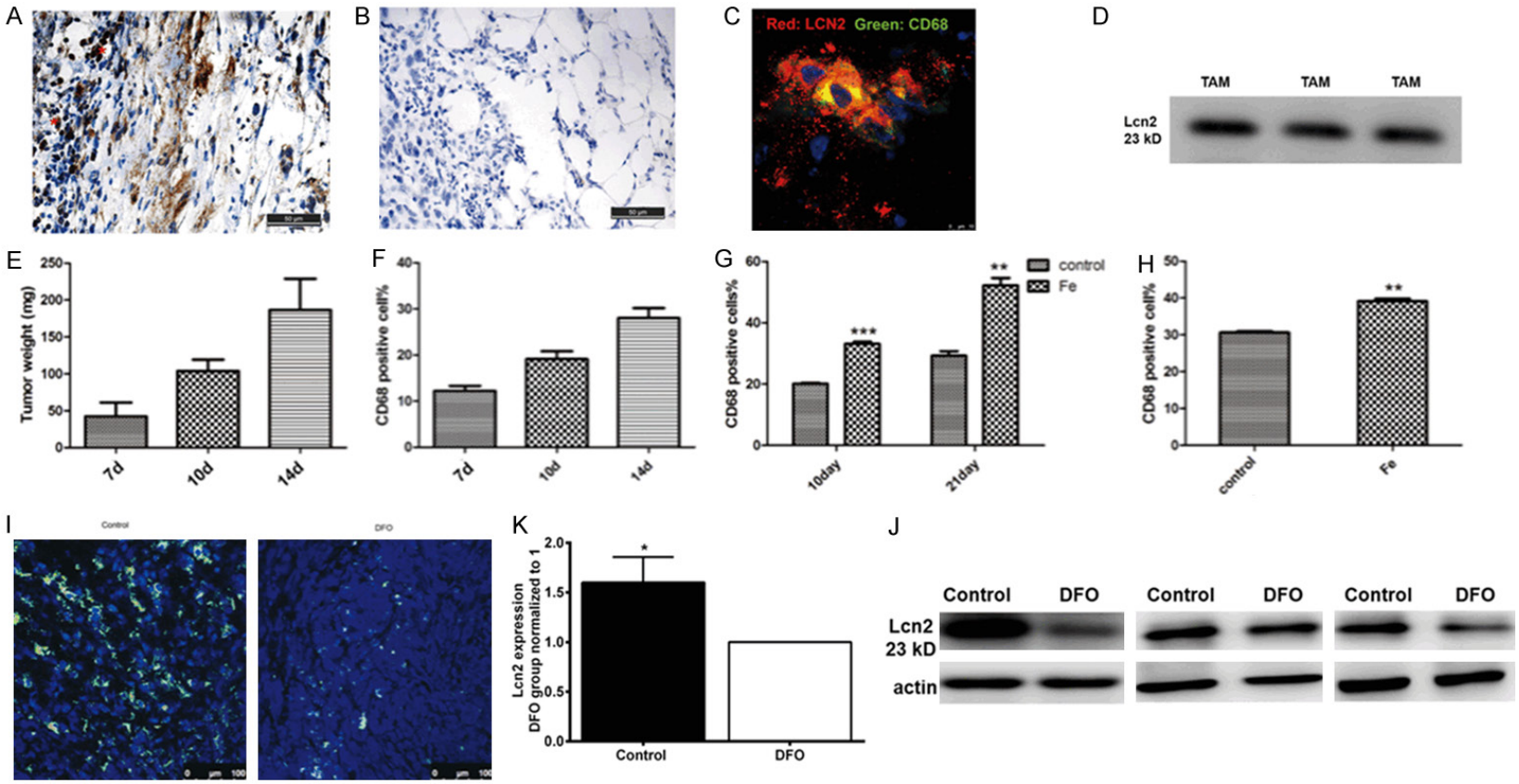

Figure 3. TAMs colocalized with Lcn2 and secreted Lcn2. A. Immunohistochemical staining of Lcn2 (asterisk marks) in the peripheral region of tumor. B. Isotype IgG was used to address the specificity of Lcn2 primary antibody. Scale bar, 50 μm. C. Co-localization of CD68 positive TAMs and Lcn2. Scale bar, 10 μm. red: Lcn2, green: CD68, blue: DAPI. D. Lcn2 was detected in TAMs culture medium by western blot. Three lanes represented three replicates. E. *Tumor weights were* evaluated on different days *after tumor inoculation*. F. Percentage of TAMs in tumors tissue at different growth stages. G. Percentage of TAMs after intraperitoneal injection of iron dextran. H. Percentage of TAMs in *in situ* breast cancer model. I. immunofluorescense staining of CD68 in tumor tissues from control group and DFO group. J, K. The expression of Lcn2 in control and DFO group detected by western blot and the results were repeated three times. n=3. Data was shown as mean ± SD. *P<0.05, **P<0.01 by Student's *t*-test.

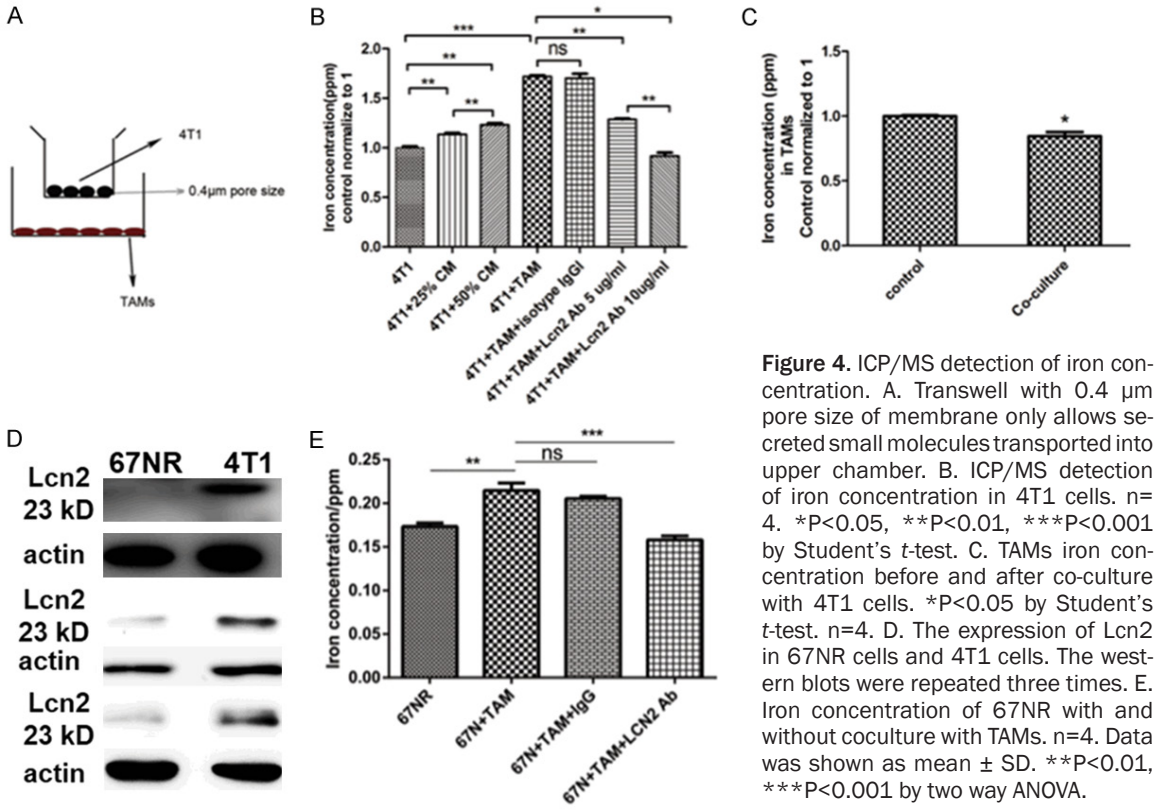

Figure 4. ICP/MS detection of iron concentration. A. Transwell with 0.4 μm pore size of membrane only allows secreted small molecules transported into upper chamber. B. ICP/MS detection of iron concentration in 4T1 cells. n= 4. *P<0.05, **P<0.01, ***P<0.001 by Student's *t*-test. C. TAMs iron concentration before and after co-culture with 4T1 cells. *P<0.05 by Student's *t*-test. n=4. D. The expression of Lcn2 in 67NR cells and 4T1 cells. The western blots were repeated three times. E. Iron concentration of 67NR with and without coculture with TAMs. n=4. Data was shown as mean ± SD. **P<0.01, ***P<0.001 by two way ANOVA.

increased nearly two-fold, which was in accordance with high iron accumulation in tumor tissues. As an alternative transporter of iron, Lcn2 could act as a potential iron transporter at tumor metastatic stage and mediate iron accumulation.

Lcn2 was originated from TAMs in the tumor microenvironment

As Lcn2 is a small molecule secretory protein, the question which types of cells in tumor tissues secreted Lcn2 was addressed. Immunohistochemical staining of Lcn2 was performed in the peripheral tumor tissues (**Figure 3A**, **3B**). The results showed that some mononuclear cells in the peripheral area expressed Lcn2 (**Figure 3A**, red asterisk marks). Moreover, immunofluorescent staining of CD68, one of macrophage markers, was utilized to identify whether these mononuclear cells were TAMs. Around the mononuclear cells, the staining of Lcn2 was overlapped with the CD68 staining (**Figure 3C**), which indicated that the mononuclear cells with strongly expressed Lcn2 were macrophages. To further identify whether TAMs secreted Lcn2, western blot analysis revealed that Lcn2 was positively detected in TAMs culture medium (**Figure 3D**). All the above results indicated that TAMs located in the invasive front of tumors secreted Lcn2.

Iron regulated feedback loop of Lcn2 in TAMs

Since tumor cells have elevated iron demand with the tumor progression, hypothetically more TAMs should be recruited into tumor tissues to provide extra iron. It was demonstrated by flow cytometry that the percentage of TAMs in tumor tissues was increased along with tumor growth (**Figure 3E**, **3F**). Systemic iron-overloaded mice model was established by intraperitoneal injection of iron dextran every third day for 4 weeks before tumor inoculation. We found that iron overload could enhance the recruitment of TAMs on day 10 (64.7%) and day 21 (78.3%) after tumor inoculation respectively in contrast to that of the control group (**Figure 3G**). To further demonstrate that iron overload induced the recruitment of TAMs, *in situ* breast cancer model was established and the results were similar: iron overload increased TAMs density in tumor tissues (**Figure 3H**). Moreover, iron depletion by iron chelator DFO administration

in vivo inhibited the recruitment of TAMs to primary tumor tissues (**Figure 3I**). Furthermore, iron chelator DFO obviously down-regulated the expression of Lcn2 in tumor tissues (**Figure 3J**, **3K**). All the above results indicated that TAMs infiltration and the expression of Lcn2 could be regulated by iron concentration, and there seemed to be a positive feed-back loop among iron, TAMs infiltration and Lcn2 secretion.

TAMs provided iron to tumor cells through Lcn2

The question whether the infiltrated TAMs in tumor tissues could provide iron to tumor cells via Lcn2 was addressed. The transwells with 0.4 μm pore size membrane were used to co-culture 4T1 cells with TAMs which avoids direct contact between two cell lines (**Figure 4A**). In this system, only secreted molecules could be transported through membrane between upper and lower chambers. When 4T1 cells were co-incubated with TAMs, iron concentration in 4T1 cells was increased by 43.34% (**Figure 4B**). After being co-incubated with 4T1 cells, iron concentration in TAMs was significantly decreased (**Figure 4C**). In addition, supplementation of 25% or 50% conditioned medium (CM) from TAMs could increase iron concentration in 4T1 cells by 13.53% or 23.32%, respectively (**Figure 4B**). Moreover, neutralization with Lcn2 antibody blunted iron concentration in a dose-dependent manner (**Figure 4B**). Antibody blocking experiment provided direct evidence that the secreted Lcn2 from TAMs could donate iron to tumor cells. In order to further demonstrate that the secreted Lcn2 from TAMs mediated iron transportation to tumor cells, we used another murine breast cancer cell line 67NR, which showed no Lcn2 expression (**Figure 4D**). After co-culture with TAMs, iron concentration of 67NR cells was significantly increased, which indicated that TAMs donated iron to 67NR cells, then Lcn2 neutralization with Lcn2 antibody impaired the iron donation (**Figure 4E**), which indicated that TAM-secreted Lcn2 mediated increase of intracellular iron. All above results indicated that TAMs provided extra iron to tumor cells via Lcn2.

Discussion

Iron overload is known to be associated with cancer risk in humans. However, little is known about the mechanism of iron accumulation in tumor metastasis. In the present study, we found that iron concentration was drastically increased at tumor metastatic stage, and iron was generally localized in the invasive front of tumors. Further studies revealed that in the tumor microenvironment, TAMs could provide extra iron to tumor cells via Lcn2.

As an important stromal component of the tumor microenvironment, macrophages are persistently recruited into the tumor stroma [19]. With the tumor progression, macrophages can be educated by tumor cells and differentiate into TAMs, which present generally M2-like phenotype [20]. And it has been demonstrated that M2 polarization is characterized by elevated activity of uptake and degradation of heme [21]. The expression of FPN and the secretion of ferritin in M2 macrophage are elevated, which indicates that M2 macrophage has enlarged iron absorption and can release iron into tumor tissues [9]. Consistent with the previous studies, we found that TAMs were most localized at the tumor margin and TAMs did have the capacity to provide iron to tumor cells. Last but not the least, the present study revealed that TAMs provided iron to tumor cells through the secreted Lcn2, which would be a third pathway besides up-regulation of FPN and the release of ferritin as reported.

However, it is very hard to identify which is the earlier event in between TAMs infiltration and increased iron concentration in tumor cells [6]. Based on our results, we regarded that the tumor microenvironment was prerequisite. In the context of the tumor microenvironment, iron could induce up-regulation of Lcn2 expression in macrophages. The tumor microenvironment evolves with the tumor progression. Tumor cells could educate menschymal cells, like macrophages, and transform them into pro-tumor phenotype, like tumor associated macrophages (TAMs), which involved in direct cell-cell interaction and cytokine networks. Among them, supplying essential nutrients meets the need of the proliferation of the malignant cancer cells is as the driving force of this transformation. Cancer cells have higher proliferative rate so that they need more iron to meet the metabolic needs, such as energy metabolism and DNA synthesis. The excess demand for iron makes cancer cells in a status of relative iron deficiency [22]. Thus, the signal

of "iron-deficiency" of cancer cells seemed to be the driving force for the infiltration of TAMs and the formation of tumor favoring microenvironment. It was the tumor microenvironment that affected the release of Lcn2 from macrophages. In the local tumor microenvironment, the high demand for iron would trigger certain cytokines release from tumor cells, which induced local TAMs to secret Lcn2 providing extra iron to tumor cells. And on the other hand, it has been indicated that Lcn2 may enhance its own expression by promoting local inflammation, which suggest an autocrine pattern of Lcn2 production in the tumor microenvironment [23]. Then more iron was provided to meet the metabolic demand of tumor cells. The positive feedback loop between iron demand and iron release of TAMs mediated by Lcn2 would be existed in the tumor microenvironment.

In the present study, we added evidence to the role of TAMs in iron delivering to tumor cells via Lcn2, although the underlying mechanism still needs to be investigated in the future study. Targeting Lcn2 secretion of TAMs to "starve cancer cells" could act as alternative option for tumor therapy.

Acknowledgements

This work was performed at the BL15U beamline of the Shanghai Synchrotron Radiation Facility (SSRF) in China, and supported by National Natural Science Foundation of China (U1532116, 11275126).

Disclosure of conflict of interest

None.

Abbreviations

TAM, tumor associated macrophage; Lcn2, Lipocalin2; EMT, epithelial-mesenchymal transition; TfR, transferrin receptor; FPN, Ferroportin; ICP-MS, Inductively coupled plasma mass spectrometry; SXRF, synchrotron radiation X-ray fluorescence; PET/CT, Positron emission tomography-computed tomography; ER stress, Endoplasmic Reticulum stress; DFO, deferoxamine; Holo-Lcn2, iron saturated Lcn2; apo-Lcn2, empty Lcn2.

Address correspondence to: Dr. Ping Liu, School of Biomedical Engineering, Shanghai Jiao Tong University, Room 400, No. 3 building, Med-X Research Institute, Shanghai Jiao Tong University No. 1954 Huashan Road, Shanghai 200030, China. Tel: (86)2162932304; E-mail: pingliu@sjtu.edu.cn

References

[1] Huang X. Iron overload and its association with cancer risk in humans: evidence for iron as a carcinogenic metal. Mutat Res 2003; 533: 153-171.

[2] Gaur A, Collins H, Wulaningsih W, Holmberg L, Garmo H, Hammar N, Walldius G, Jungner I and Hemelrijck MV. Iron metabolism and risk of cancer in the Swedish AMORIS study. Cancer Causes Control 2013; 24: 1393-1402.

[3] Pinnix ZK, Miller LD, Wang W, D'Agostino R Jr, Kute T, Willingham MC, Hatcher H, Tesfay L, Sui G, Di X, Torti SV, Torti FM. Ferroportin and iron regulation in breast cancer progression and prognosis. Sci Transl Med 2010; 2: 43ra56.

[4] Majewska U, Banaś D, Braziewicz J, Góźdź S, Kubala-Kukuś A and Kucharzewski M. Trace element concentration distributions in breast, lung and colon tissues. Phys Med Biol 2007; 52: 3895.

[5] Torti SV and Torti FM. Iron and cancer: more ore to be mined. Nat Rev Cancer 2013; 13: 342-355.

[6] Jung M, Mertens C and Brüne B. Macrophage iron homeostasis and polarization in the context of cancer. Immunobiology 2015; 220: 295-304.

[7] Theerauwut Chanmee PO, Kenjiro Konno, Naoki Itano. Tumor-associated macrophages as major player in the tumor microenvironment. Cancers 2014; 6: 1670-1690.

[8] Tang X. Tumor-associated macrophages as potential diagnostic and prognostic biomarkers in breast cancer. Cancer Lett 2013; 332: 3.

[9] Cairo G, Recalcati S, Mantovani A and Locati M. Iron trafficking and metabolism in macrophages: contribution to the polarized phenotype. Trends Immunol 2011; 32: 241.

[10] Silva MC, Cerwenka A and Muckenthaler MU. The role of iron in cancer and in the polarization of tumor-associated macrophages. Am J Hematol 2013; 88: E183-E184.

[11] Jung M, Mertens C, Bauer R, Rehwald C and Brüne B. Lipocalin-2 and iron trafficking in the tumor microenvironment. Pharmacol Res 2017; 120: 146.

[12] Mertens C, Akam EA, Rehwald C, Brüne B, Tomat E and Jung M. Intracellular iron chelation modulates the macrophage iron phenotype with consequences on tumor progression. PLoS One 2016; 11: e0166164.

[13] Jung M, Weigert A, Tausendschön M, Mora J, Ören B, Sola A, Hotter G, Muta T and Brüne B. Interleukin-10-induced neutrophil gelatinase-associated lipocalin production in macrophages with consequences for tumor growth. Mol Cell Biol 2012; 32: 3938-3948.
[14] Pulaski BA and Ostrand-Rosenberg S. Mouse 4T1 breast tumor model. Curr Protoc Immunol 2001; Chapter 20: Unit 20.2.
[15] Tao K, Fang M, Alroy J and Sahagian GG. Imagable 4T1 model for the study of late stage breast cancer. BMC Cancer 2008; 8: 228.
[16] Li CY, Shan S, Huang Q, Braun RD, Lanzen J, Hu K, Lin P and Dewhirst MW. Initial stages of tumor cell-induced angiogenesis: evaluation via skin window chambers in rodent models. J Natl Cancer Inst 2000; 92: 1445-1446.
[17] Xie Y, Li J, Liu P, Xu LX and Zhang J. Trace metal distribution and correlation to breast cancer progression and metastasis based on synchrotron radiation X-ray fluorescence imaging. International Conference on Biomedical Engineering and Biotechnology 2012.
[18] Rodvold JJ, Mahadevan NR and Zanetti M. Lipocalin 2 in cancer: when good immunity goes bad. Cancer Lett 2012; 316: 132-138.
[19] Shieh YS, Hung YJ, Hsieh CB, Chen JS, Chou KC and Liu SY. Tumor-associated macrophage correlated with angiogenesis and progression of mucoepidermoid carcinoma of salivary glands. Ann Surg Oncol 2009; 16: 751.
[20] Lewis CE and Pollard JW. Distinct role of macrophages in different tumor microenvironments. Cancer Res 2006; 66: 605-612.
[21] Kroner A, Greenhalgh AD, Zarruk JG, Passos DS, Gaestel M and David S. TNF and increased intracellular iron alter macrophage polarization to a detrimental M1 phenotype in the injured spinal cord. Neuron 2014; 83: 1098.
[22] Wang W, Deng Z, Hatcher H, Miller LD, Di X, Tesfay L, Sui G, D'Agostino RB, Torti FM and Torti SV. IRP2 regulates breast tumor growth. Cancer Res 2014; 74: 497-507.
[23] Leng X, Wu Y and Arlinghaus RB. Relationships of lipocalin 2 with breast tumorigenesis and metastasis. J Cell Physiol 2011; 226: 309-314.